Probabilistic analysis of tumor growth inhibition models to Support trial design

Citation for the original published paper (version of record):
Baaz, M., Cardilin, T., Lundh, T. et al (2024). Probabilistic analysis of tumor growth inhibition models to Support trial design. Journal of Theoretical Biology, 595.
http://dx.doi.org/10.1016/j.jtbi.2024.111969

Journal of Theoretical Biology 595 (2024) 111969

Contents lists available at ScienceDirect

Journal of Theoretical Biology

journal homepage: www.elsevier.com/locate/yjtbi

Probabilistic analysis of tumor growth inhibition models to Support trial design

Marcus Baaz [a,b,*], Tim Cardilin [a], Torbjörn Lundh [b], Mats Jirstrand [a]

[a] Fraunhofer-Chalmers Research Centre for Industrial Mathematics, Gothenburg, Sweden
[b] Department of Mathematical Sciences, Chalmers University of Technology and University of Gothenburg, Gothenburg, Sweden

ARTICLE INFO

Keywords:
Power Analysis
Combination Therapy
Oncology
Nonlinear Mixed Effects
Mathematical modeling

ABSTRACT

A large enough sample size of patients is required to statistically show that one treatment is better than another. However, too large a sample size is expensive and can also result in findings that are statistically significant, but not clinically relevant. How sample sizes should be chosen is a well-studied problem in classical statistics and analytical expressions can be derived from the appropriate test statistic. However, these expressions require information regarding the efficacy of the treatment, which may not be available, particularly for newly developed drugs. Tumor growth inhibition (TGI) models are frequently used to quantify the efficacy of newly developed anticancer drugs. In these models, the tumor growth dynamics are commonly described by a set of ordinary differential equations containing parameters that must be estimated using experimental data.

One widely used endpoint in clinical trials is the proportion of patients in different response categories determined using the Response Evaluation Criteria In Solid Tumors (RECIST) framework. From the TGI model, we derive analytical expressions for the probability of patient response to combination therapy. The probabilistic expressions are used together with classical statistics to derive a parametric model for the sample size required to achieve a certain significance level and test power when comparing two treatments.

Furthermore, the probabilistic expressions are used to generalize the Tumor Static Exposure concept to be more suitable for predicting clinical response. The derivatives of the probabilistic expressions are used to derive two additional expressions characterizing the exposure and its sensitivity. Finally, our results are illustrated using parameters obtained from calibrating the model to preclinical data.

1. Introduction

Cancer is one of the leading causes of death globally and the number of cases is expected to increase due to the world's aging population (Sung et al., 2021). Fortunately, a lot of resources are being invested to find new and improved treatments. This has not only resulted in the prolongation of lives but has also enabled curative treatment for certain types of cancer that used to be incurable (Jacobs, 1997; Broxmeyer, 2020). These improvements are partially due to the usage of combination therapies, which is defined as the concomitant administration of two or more drugs or treatment modalities (Hemminki et al., 2023).

All individuals do not respond the same way to treatment and it is thought that this between-subject variability (BSV) in response is one of the reasons for the benefit of combination therapies over monotherapies (Palmer and Sorger, 2017). Moreover, when combining drugs there is also the possibility of synergistic drug effects (Al-Lazikani et al., 2012). However, identifying drug combinations with sufficient clinical efficacy early in the drug development process is still a challenging task (Park et al., 2004). Mathematical modeling can provide insights into what drug has the highest potential for clinical success by, *e.g.,* quantifying BSV and other types of variability (Yin et al., 2019; Koga and Ochiai, 2019), which is often done in pharmacometrics using tumor growth inhibition (TGI) models and the nonlinear mixed effects (NLME) framework (Ribba et al., 2012; Leander et al., 2021).

An important objective of mathematical modeling is finding threshold values, or target exposures, that when exceeded, are predicted to lead to a specific treatment outcome (Koch et al., 2009; Goteti et al., 2010; Miao et al., 2016). One commonly used target exposure is the so-called Tumor Static Exposure (TSE) (Jumbe et al., 2010; Gabrielsson et al., 2016; Cardilin et al., 2017). TSE is defined as all exposure that results in tumor stasis and therefore separates the space of all exposures into a region of tumor growth and a region of tumor shrinkage.

* Corresponding author.
E-mail address: Marcus.Baaz@fcc.chalmers.se (M. Baaz).

https://doi.org/10.1016/j.jtbi.2024.111969
Received 22 December 2022; Received in revised form 8 May 2024; Accepted 10 October 2024
Available online 18 October 2024

However, because of this separation into two regions, TSE does not fully correspond to the well-established Response Evaluation Criteria In Solid Tumors (RECIST) classification, where patients' response is measured using four categories; progressive disease (PD), stable disease (SD), partial response (PR), and complete response (CR) (Eisenhauer et al., 2009).

In this paper, we aim to find analytical expressions that describe the probability of RECIST classification, *i.e.,* the proportion of patients in each RECIST category, using a TGI model based on ordinary differential equations (ODEs). Since the model does not explicitly predict tumor eradication we combine CR and PR into a single category. This combined category is commonly referred to as objective response rate (Zettler et al., 2021). To adequately deal with BSV we use the NLME framework and focus on the often used log-normal distribution (Ouerdani et al., 2015). We combine the results from this analysis with classical statistics to predict the necessary sample size required to achieve a certain significance level and test power when comparing two treatments.

Moreover, we extend the TSE concept to better correspond to the RECIST classification and allow for more informative clinical predictions. Sensitivity equations along with two other potentially interesting exposures are also derived. The first of these describes the exposure combinations that maximize the number of individuals categorized as SD and the other those combinations for which the number of individuals in the CR&PR category is increased the most. Finally, to illustrate our results, we calibrate the model to preclinical xenograft data.

1.1. Tumor growth inhibition model

The exponential tumor growth model is often used to describe the dynamics of tumor cells when an individual is given a combination of different drugs (Yin et al., 2019; Choo et al., 2013; Ribba et al., 2014). If we assume that M drugs are given simultaneously and the monotherapy efficacy of the drugs is described by linear functions and the drug interactions by quadratic terms, the turnover of tumor cells is given by,

$$\frac{dTS(t)}{dt} = \left(k_g - \Sigma_{i=1}^{M} a_i C_i(t) - \Sigma_{i=1}^{M}\Sigma_{j=1}^{M}\gamma_{ij} C_i(t) C_j(t)\right) TS(t), TS(0) = TS_0, \tag{1}$$

where TS is the tumor size, TS_0 the initial tumor size, $k_g \geq 0$ the tumor growth rate before start of treatment, and $a_i \geq 0$ and $C_i \geq 0$ the potency and concentration of drug i at time t, respectively. The parameters γ_{ij} describe the type and strength of the interaction effects between drugs i and j, with $\gamma_{ij} = 0, \gamma_{ij} > 0$ and $\gamma_{ij} < 0$ indicating an additive, synergic, and antagonistic combination, respectively. For $i = j$ we always have $\gamma_{ij} = 0$.

The analytical solution to Eq. (1) is,

$$TS(t) = TS_0 e^{\int_0^t k_{g,nt}(\tau)\,\mathrm{d}\tau}, \tag{2}$$

where,

$$k_{g,nt}(\mathrm{t}) = k_g - \Sigma_{i=1}^{M} a_i C_i(t) - \Sigma_{i=1}^{M}\Sigma_{j=1}^{M}\gamma_{ij} C_i(t) C_j(t).$$

The time dependence of $k_{g,nt}$ is due to the drug dynamics' and the treatment schedule. If we assume no interaction effects, then the exponent in Eq. (2) is,

$$\int_0^t k_{g,nt}(\tau)\,\mathrm{d}\tau = k_g t - \Sigma_{i=1}^{M} a_i \int_0^t C_i(\tau)\,\mathrm{d}\tau$$

For any concentration profile, the integral of C_i is commonly referred to as the area under the curve ($AUC_{i,0-t}$) of drug i, hence the entire integral can be written as,

$$\int_0^t k_{g,nt}(\tau)\,\mathrm{d}\tau = k_g t - \Sigma_{i=1}^{M} \frac{a_i AUC_{i,0-t} t}{t} = (k_g - \Sigma_{i=1}^{M} a_i \overline{C_i}) t$$

where $\overline{C_i}$ is the average concentration of drug i. If we consider the case with interaction effects we will get terms on the following form, $\int_0^t \gamma_{ij} C_i(\tau) C_j(\tau)\mathrm{d}\tau$. Here, pharmacokinetic models of both drugs and the treatment schedule must be considered to solve to the integral. However, the general form it will take is,

$$\int_0^t \gamma_{ij} C_i(\tau) C_j(\tau)\mathrm{d}\tau = \gamma_{ij} AUC_{ij}(t).$$

Thus, as we saw before, the potency terms will always consist of average concentrations, whereas the interaction terms have more complicated expressions. We compute the integrals for specific choices of pharmacokinetic models in the Appendix. The upcoming analysis can be performed in keeping with the exact expressions, however, in practice, letting the average concentration drive the pharmacodynamic response is often a reasonable modeling choice. Furthermore, given two concentration models, $AUC_{ij}(t)$ will simply be a single scalar value, since we later fix the time. Due to both of these reasons, we let $C_i(t) = \overline{C_i}$. Under this assumption, the interaction term integral becomes $\gamma_{ij}\overline{C_i}\overline{C_j}t$. For simplicity's sake, we henceforward denote $\overline{C_i}$ with C_i. The system we analyze thus becomes,

$$\frac{dTS(t)}{dt} = (k_g - S) TS(t), TS(0) = TS_0, \tag{3}$$

$$S = \Sigma_{i=1}^{M} a_i C_i - \Sigma_{i=1}^{M}\Sigma_{j=1}^{M}\gamma_{ij} C_i C_j$$

with the analytical solution,

$$TS(t) = TS_0 e^{(k_g - S)t} \tag{4}$$

To account for BSV we use the NLME framework, where some of the model parameters are assumed to follow a distribution across the population. In this paper, we focus on parameters that are log-normally (LN) distributed as this often is the first choice in pharmacometrics. However, the result from many mathematical operations between log-normally distributed variables, *e.g.,* addition or subtraction, have intractable Cumulative Distribution Functions (CDFs) (Ben Hcine, 2014). This means that for the analytical analysis, we can only consider the case with a single log-normally distributed parameter in the ODE part of Eq. (3). To be able to capture the dynamics of both untreated and treated individuals we choose this parameter to be k_g.

In general, any log-normally distribution parameter, θ, can be represented in the following manner,

$$\theta = \theta^m e^{\eta}$$

where θ^m is the median population value and $\eta \sim N(0, \omega^2)$.

1.2. Modeling of preclinical data

Gao *et al.* have published a large dataset where different drug combinations were tested in patient-derived xenograft (PDX) mice (Gao et al., 2015). From this publication, we used tumor volume time series data from the trial where PDXs, established from patients with colorectal cancer (CRC), were either untreated (N = 45) or given BYL719 and binimetinib as either mono (N = 44 in both arms) or combination therapy (N = 43). 10 mg/kg doses of binimetinib were administered orally twice daily for both treatment arms. This treatment schedule has been tested in rats previously and it was found that the average concentration was approximately 12 $\mu g/mL$ (Center for Drug Evaluation and Research. Multi-Disciplinary Review and Evaluation NDA, 2015). BYL719 was also given orally, but with daily doses of 50 mg/kg and 25

mg/kg for the monotherapy and combination therapy treatment arms, respectively. We perform a linear extrapolation of the average concentration based on previous findings in both humans and rats and found that these treatment schedules give approximately an average concentration of 5.6 $\mu g/mL$ and 2.8 $\mu g/mL$, respectively. (Center for Drug Evaluation and Research. Pharmacology Review of Alpelisib., 2018).

The standard dosing time was 21 days and, therefore, we only use data up to this day. All data is shown in Fig. 1 and to analyze the data we use the model presented in Eq. (3) with C_1 and C_2 being the average concentration of binimetinib and BYL719, respectively.

Using Monolix, a maximum likelihood approach utilizing the Stochastic Approximation Expectation Maximization algorithm (SAEM) is used to obtain the parameter estimates (Delyon et al., 1999; Monolix, 2021). k_g and TS_0 are assumed to be uncorrelated and log-normally distributed with medians given by k_g^m and TS_0^m and standard deviations by ω_{k_g} and ω_{TS_0}. A proportional zero-mean normally distributed error term, with standard deviations s is used to describe the difference between the model predictions and the data. The model fit is validated based on the precision of parameter estimates, individual fits, likelihood values, and residual plots.

1.3. Clinical RECIST Categorization

In clinical oncology studies, patients' response is categorized using RECIST (Eisenhauer et al., 2009). The tumor size, in terms of the sum of the longest diameters (SLD) for all target lesions, is measured at the start of treatment (baseline) and at subsequent checkups, typically every 6 or 8 weeks. How much the tumor has grown or shrunk at time T from the baseline is calculated according to,

$$\rho = 100\%\frac{TS(T) - TS_{baseline}}{TS_{baseline}}. \tag{5}$$

During check-ups, patients are classified as CR&PR if $\rho \leq -30\%$, as PD if $\rho \geq 20\%$, and as SD otherwise. Since TS is influenced by the parameters' distributions it is a random variable. Consequently, ρ is also a random variable and by considering its CDF at $t = T$, the probability of classification at a chosen time point, denoted as $P_{\text{CR\&PR}}$, P_{PD} and P_{SD}, can be obtained.

It should be noted that this is only based on the criteria for the target lesion progression and for PD it is the nadir measurement that is used instead of the baseline. However, in the model, the nadir and baseline values are the same for an individual with disease progression.

1.4. Sample size predictions

Denote the proportion of patients classified as CR&PR in two independent studies (same sample size) by p_1 and p_2. The sample size required to show an ϵ difference between p_1 and p_2 is given by,

$$n = \frac{\left(z_{\frac{\alpha}{2}} + z_{\beta}\right)^2}{\epsilon^2}(p_1(1-p_1) + p_2(1-p_2)), \tag{6}$$

where z is the standard score, α the confidence level, and $1-\beta$ the power of the test (Sakpal, 2010; Wang and China, 2007).

1.5. Target exposure

To illustrate the classical TSE concept, we consider Eq. (3) with two drugs ($M = 2$). We solved the ODE with the right-hand side equal to zero

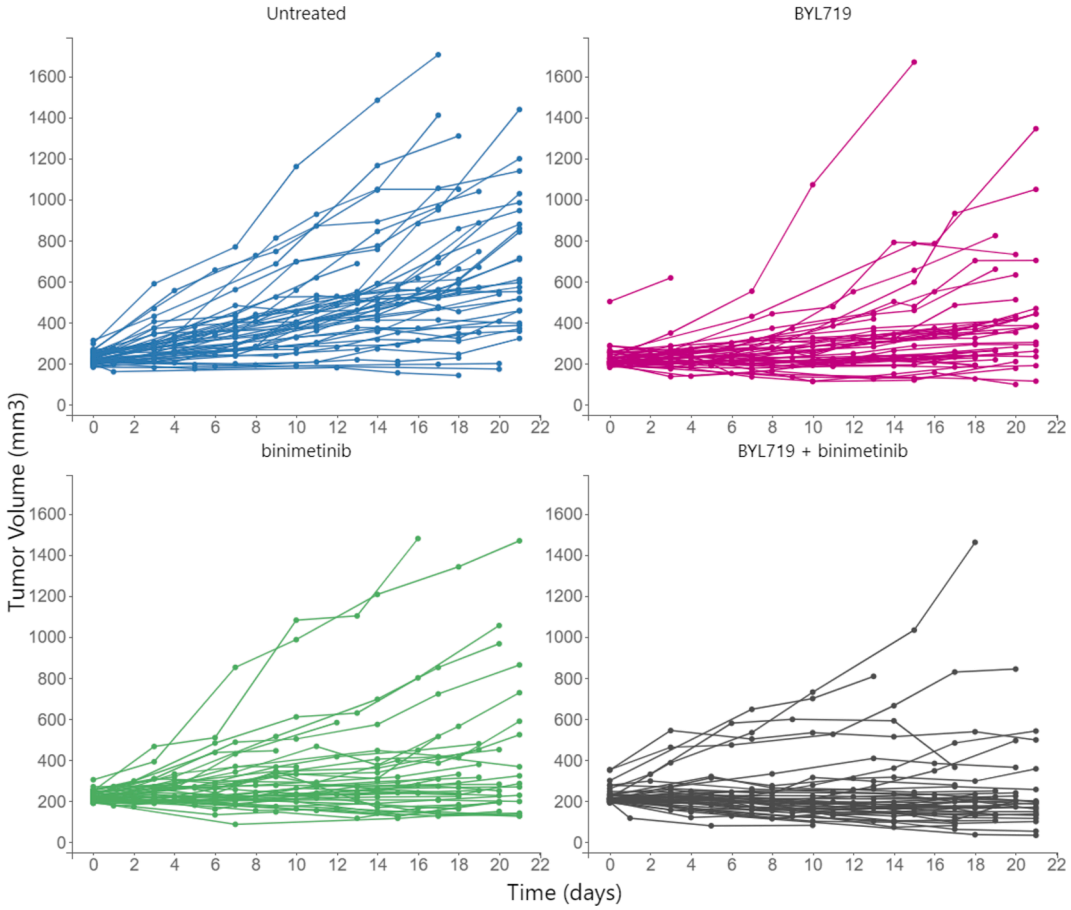

Fig. 1. Tumor volume time series of PDX mice.

to find the median TSE equation for this model. From this, we solve for one of the concentrations, *e.g.*, C_2, and arrive at the following expression describing the necessary C_2 to induce tumor stasis as a function of C_1 and the model parameters,

$$C_2 = \frac{(k_g - a_1 C_1)}{\gamma_{12} C_1 + a_2}. \tag{7}$$

An example of a TSE curve is shown on the left side of Fig. 4. However, this equation is not affected by the treatment period, and can thus be problematic to use for predicting clinical efficacy.

2. Results

In this section, the parameter estimates from the modeling are first shown. Next a lemma that gives analytical expressions for the probability of classification to each RECIST category is presented and a proof of it can be found in the Appendix. This lemma is then used to state and prove a theorem detailing how one can predict the necessary sample size of a study to show a difference between two treatments with a specific significance level and test power. Following this, an extended version of the classical TSE concept, that incorporates the treatment period, is derived. Finally, we also present two target exposure equations for guiding study design along with sensitivity equations.

2.1. Modeling

The model was able to describe the data well and individual fits (A.1-A.4), observation versus predictions plot (A.5), and residual plots (A.6) are found in the Appendix. Furthermore, all parameters were estimated with good precision, in terms of relative standard errors (RSE), and are shown in Table 1.

2.2. RECIST probability

The probability of satisfying the criteria for each RECIST category can be found by first combining Eqs. (4) and (5), which leads to,

$$\rho = 100\%\left(\frac{TS_0 e^{(k_g - S)t} - TS_0}{TS_0}\right) = 100\%\left(e^{(k_g - S)t} - 1\right). \tag{8}$$

Next, we need to evaluate the CDF of ρ. Note that since the initial tumor size cancels out in Eq. (8), the upcoming result is applicable for any reasonable assumption of its distribution. For simplicity's sake, we will assume that it is constant. Hence, we also drop the index from ω_{k_g} and let ω be the standard deviation of k_g in the analytical analysis. Throughout the paper we let Φ denote the CDF of the standard normal distribution, *i.e.*,$N(0,1)$.

Lemma 1. *Assume a TGI model with tumor dynamics given by Eq. (3), where* $k_g \sim LN(\log(k_g^m), \omega)$. *Then the probability of being classified to each of the three response categories at time* $t = T$ *can be expressed as,*

$$P_{\text{CR\&PR}} = \chi_{\frac{\log(0.7)}{T}+S>0}\,\Phi\left(\log\left(\frac{\frac{\log(0.7)}{T}+S}{k_g^m}\right)/\omega\right),$$

$$P_{PD} = 1 - \Phi\left(\log\left(\frac{\frac{\log(1.2)}{T}+S}{k_g^m}\right)\Big/\,\omega\right), \tag{9}$$

$$P_{SD} = \Phi\left(\frac{\log\left(\frac{\frac{\log(1.2)}{T}+S}{k_g^m}\right)}{\omega}\right) - \chi_{\frac{\log(0.7)}{T}+S>0}\,\Phi\left(\frac{\log\left(\frac{\frac{\log(0.7)}{T}+S}{k_g^m}\right)}{\omega}\right).$$

A proof of the lemma can be found in the Appendix. The three probabilities in Lemma 1 are shown in Fig. 2, as functions of the average concentration, for the binimetinib monotherapy group with $t = 21$ *days* along with the parameters from Table 1. We can see that $P_{CR\&PR}$ and P_{PD} are both monotone functions. However, this is not the case for P_{SD} with these parameter values.

Theorem 1. *Assume that the efficacy of M drugs is being compared with the efficacy of the same M drugs minus one of the drugs, that the tumor dynamics be provided by Eq. (3), where* $k_g \sim LN(\log(k_g^m), \omega)$ *and* $\frac{\log(0.7)}{T} + S > 0$. *Then the predicted sample size required, n, to show an* $\epsilon = \Phi(z_2) - \Phi(z_1)$ *difference in objective response rate between the two treatments at the end of the trial, with a significance level of* α *and power* $1-\beta$, *is given by,*

$$n = \frac{\left(z_{\frac{\alpha}{2}} + z_\beta\right)^2 (\Phi(z_1)(1-\Phi(z_1)) + \Phi(z_2)(1-\Phi(z_2)))}{(\Phi(z_2) - \Phi(z_1))^2},$$

or

$$n = \frac{\left(z_{\frac{\alpha}{2}} + z_\beta\right)^2 \left(\frac{\pi}{2} - \left(\int_0^{\frac{z_1}{\sqrt{2}}} e^{-t^2} dt\right)^2 - \left(\int_0^{\frac{z_2}{\sqrt{2}}} e^{-t^2} dt\right)^2\right)}{\left(\int_0^{\frac{z_2}{\sqrt{2}}} e^{-t^2} dt - \int_0^{\frac{z_1}{\sqrt{2}}} e^{-t^2} dt\right)^2}, \tag{10}$$

where $z_1 = \log\left(\frac{\frac{\log(0.7)}{T} + \sum_{i=1}^{M-1} a_i C_i + \sum_{i=1}^{M-1}\sum_{j=1}^{M-1} \gamma_{ij} C_i C_j}{k_g^m}\right)/\omega$ and $z_2 = \log\left(\frac{\frac{\log(0.7)}{T} + \sum_{i=1}^{M} a_i C_i + \sum_{i=1}^{M}\sum_{j=1}^{M} \gamma_{ij} C_i C_j}{k_g^m}\right)/\omega.$

Proof. *An application of Lemma 1 in combination with Eq.* (6) *and the CDF of the standard normal distribution yields the result.*∎

Fig. 3 shows an application of the theorem for testing the efficacy of binimetinib given as monotherapy versus it in combination with 2.6 $\mu g/mL$ BYL719. The significance level and test power are 95 % and 80 %, respectively. The model parameters are taken from Table 1 with $t = 21$ *days* and the concentration used in the trial is marked in red.

Table 1
Estimated parameters.

Parameter	Units	Estimate (RSE)	Description
a_1	$mL\mu g^{-1} days^{-1}$	$4 \cdot 10^{-3}$ (12)	Potency of binimetinib
a_2	$mL\mu g^{-1} days^{-1}$	$6 \cdot 10^{-3}$ (12)	Potency of BYL719
γ_{12}	$(mL\mu g^{-1} days^{-1})^2$	$5 \cdot 10^{-4}$ (17)	Interaction effect
TS_0^m	mm^3	225 (1)	Median initial tumor volume
k_g^m	$days^{-1}$	0.05 (5)	Median growth rate
ω_{TS_0}	–	0.18 (6)	Standard deviation of initial tumor volume
ω_{k_g}	–	0.57 (7)	Standard deviation of growth rate
s	–	0.12 (6)	Standard deviation of error term

2.3. Target exposure

Proposition 1. *Assume a drug combination of two drugs, tumor dynamics given by Eq. (3), where* $k_g \sim LN(\log(k_g^m), \omega)$, *and* $\frac{\log(0.7)}{T} + a_1 C_1 + a_2 C_2 + \gamma_{12} C_1 C_2 > 0$. *Then the relationship between drug exposures and a specific probability of CR&PR and PD classification,* P_x, *are*

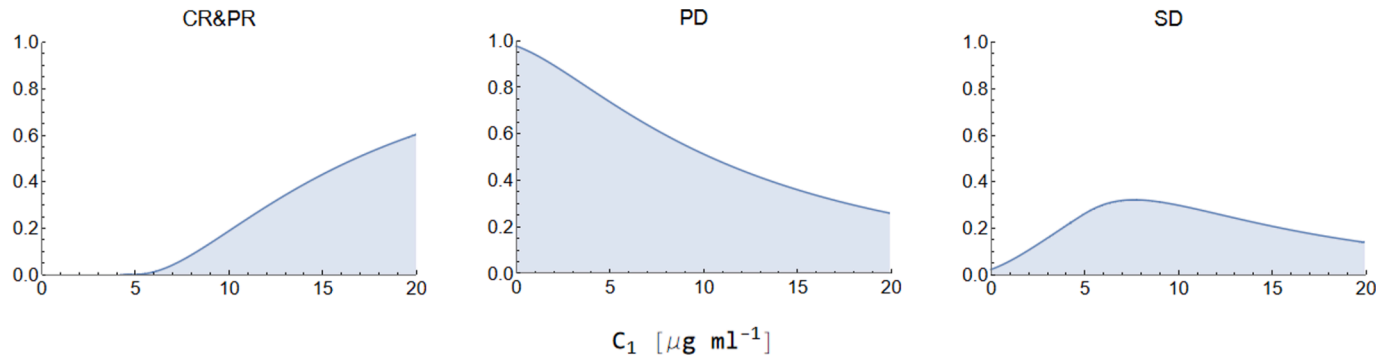

Fig. 2. RECIST Predictions. The proportion of patients classified as CR&PR, PD, and SD at $t = 21 days$ given binimetinib as monotherapy, plotted as functions of the average concentration.

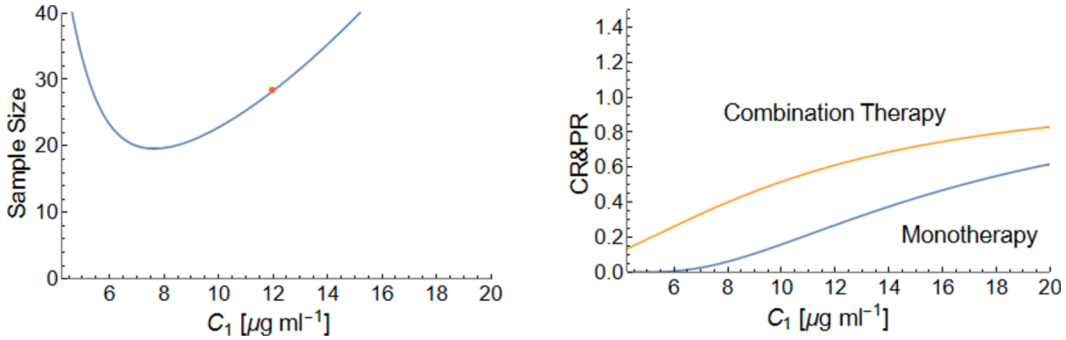

Fig. 3. Predictions of Two Treatments. (Left) The required sample size prediction for testing binimetinib given as a monotherapy against it given in combination with $2.6\mu g/mL$ BYL719. The average concentration of binimetinib used in the trial is marked with red. (Right) The predicted efficacy, in terms of the proportion of patients with CR&PR for the monotherapy (blue) and the combination therapy (yellow). (For interpretation of the references to color in this figure legend, the reader is referred to the web version of this article.)

given by,

$$C_2 = \frac{k_g^m e^{\omega Z_{P_x}} - \frac{\log(0.7)}{T} - a_1 C_1}{a_2 + \gamma_{12} C_1}, \tag{11}$$

$$C_2 = \frac{k_g^m e^{\omega Z_{P_x}} - \frac{\log(1.2)}{T} - a_1 C_1}{a_2 + \gamma_{12} C_1}, \tag{12}$$

respectively. Here Z_{P_x} is the inverse CDF of $N(0,1)$ evaluated at P_x.

Proof. *For* $\frac{\log(0.7)}{T} + a_1 C_1 + a_2 C_2 + \gamma_{12} C_1 C_2 > 0$, *we have from* Lemma 1 *that,*

$$P_{\text{CR\&PR}} = \Phi\left(\log\left(\frac{\frac{\log(0.7)}{T} + a_1 C_1 + a_2 C_2 + \gamma_{12} C_1 C_2}{k_g^m}\right)/\omega\right)$$

Putting the probability equal to a specific value, P_x, we have,

$$P_{\text{CR\&PR}} = \Phi\left(\log\left(\frac{\frac{\log(0.7)}{T} + a_1 C_1 + a_2 C_2 + \gamma_{12} C_1 C_2}{k_g^m}\right)/\omega\right) = P_x,$$

$$\log\left(\frac{\frac{\log(0.7)}{T} + a_1 C_1 + a_2 C_2 + \gamma_{12} C_1 C_2}{k_g^m}\right)/\omega = \Phi^{-1}(P_x) = Z_{P_x}.$$

Now solving for C_2 yields the exposure for CR&PR and exchanging $\log(0.7)$ for $\log(1.2)$ gives the equation for PD.∎

Eqs. (11) and (12) are plotted together on the right side of Fig. 4, using the parameters from Table 1 and $t = 21$ *days*, for the median individual, *i.e.*, $P_x = 0.5$. Together they separate all possible exposure combinations of drugs 1 and 2 into three areas, each representing one of the RECIST categories. Eq. (11) is also shown as a heatmap in Fig. 5, with each axis representing one drug and the intensity representing the proportion classified as CR&PR.

Having equations for $P_{CR\&PR}$ also allows for its derivative to be found, which in turn permits further analysis. One might *e.g.,* be interested in knowing when it is maximized, *i.e.,* at what exposure level is an increase in drug exposure most beneficial to the patient. Conversely, it might also be of interest to know when an increase in drug exposure leads to little or no benefit to the patient. The following proposition answers the first of these questions.

Proposition 2. *Assume a drug combination of two drugs, tumor dynamics given by Eq. (3) where* $k_g \sim LN(\log(k_g^m), \omega)$, *and* $\frac{\log(0.7)}{T} + a_1 C_1 + a_2 C_2 + \gamma_{12} C_1 C_2 > 0$. *Then the exposure pairs that maximize* $\frac{dP_{CR\&PR}}{dC_i}$, $i = 1, 2$, *are given by,*

$$C_2 = \frac{k_g^m e^{-\omega^2} - \frac{\log(0.7)}{T} - a_1 C_1}{a_2 + \gamma_{12} C_1}. \tag{13}$$

Proof. *From* Lemma 1 *we have that the probability of CR&PR classification is,*

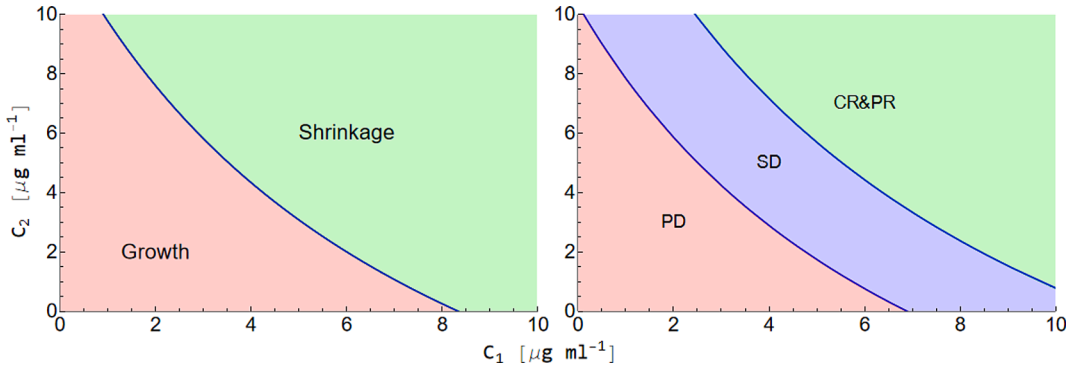

Fig. 4. Tumor Static Exposure. (Left) Illustration of the classical TSE concept. Exposure combinations on the green lead to tumor shrinkage, whilst pairs on the red lead to tumor growth. (Right) Illustration of RECIST predictions according to Proposition 1. Exposure pairs on the different colored areas are predicted to lead to the corresponding RECIST classification. (For interpretation of the references to color in this figure legend, the reader is referred to the web version of this article.)

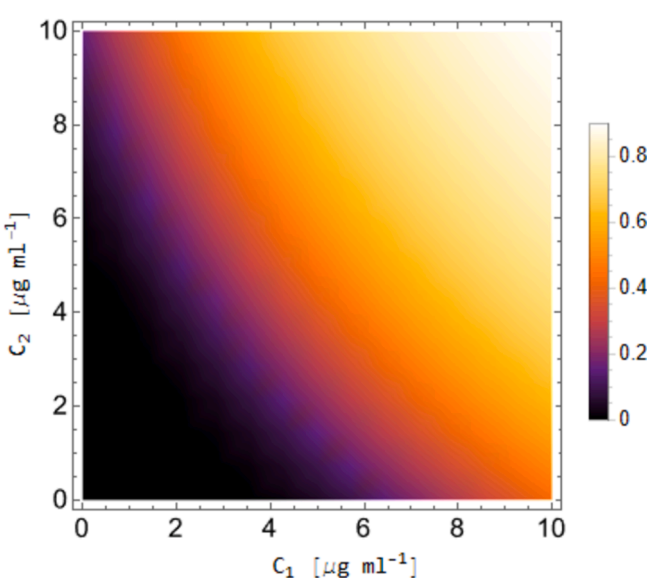

Fig. 5. CR&PR Heatmap. The proportion of patients classified as CR&PR as a heat map of the average concentration of drugs 1 and 2. Higher color intensity indicates a higher proportion of CR&PR.

$$P_{\text{CR\&PR}} = \Phi\left(\log\left(\frac{\frac{\log(0.7)}{T} + a_1C_1 + a_2C_2 + \gamma_{12}C_1C_2}{k_g^m}\right)/\omega\right).$$

Differentiating once, using that the derivative of a CDF is the corresponding PDF and the chain rule, yields.

$$\frac{dP_{CR\&PR}}{dC_1} = \frac{(a_1+\gamma_{12}C_2)e^{-\log^2\left(\frac{a_1C_1+a_2C_2+\gamma_{12}C_1C_2+\frac{\log(0.7)}{T}}{k_g^m}\right)\Big/\omega^2}}{\sqrt{2\pi}\omega\left(\frac{\log(0.7)}{T}+a_1C_1+a_2C_2+\gamma_{12}C_1C_2\right)}. \tag{14}$$

Now, to find what exposure combinations maximize Eq. (14), we differentiate again and solve it equal to zero.

$$\frac{d^2P_{CR\&PR}}{dC_1^2} = -\frac{(a_1+\gamma_{12}C_2)^2 e^{-\log^2\left(\frac{a_1C_1+a_2C_2+\gamma_{12}C_1C_2+\frac{\log(0.7)}{T}}{k_g^m}\right)\Big/2\omega^2}}{\omega\sqrt{2\pi}\left(a_1C_1+a_2C_2+\gamma_{12}C_1C_2+\frac{\log(0.7)}{T}\right)^2}\left(1 + \frac{\log\left(\frac{a_1C_1+a_2C_2+\gamma_{12}C_1C_2+\frac{\log(0.7)}{T}}{k_g^m}\right)}{\omega^2}\right)$$

$$= 0$$

$$1 + \frac{\log\left(\frac{a_1C_1+a_2C_2+\gamma_{12}C_1C_2+\frac{\log(0.7)}{T}}{k_g^m}\right)}{\omega^2} = 0$$

Solving for C_2 gives,

$$C_2 = \frac{k_g^m e^{-\omega^2} - \frac{\log(0.7)}{T} - a_1C_1}{a_2+\gamma_{12}C_1}. \tag{15}$$

Because of the symmetry between C_1 and C_2, the same equation is found if one instead solves $\frac{d^2P_{CR\&PR}}{dC_2^2} = 0$. ∎

Comparing Eqs. (11) and (15) we can see that they only equal each other when $Z_{P_x} = -\omega$, meaning that the combination of C_1 and C_2 that result in $\frac{dP_{CR\&PR}}{dC_i}$ being maximized is the same as those resulting in $P_x = \Phi(-\omega)$. In other words, let say C_1 is fixed to some value, then the C_2 that results in $P_{CR\&PR} = \Phi(-\omega)$ also results in $\frac{dP_{CR\&PR}}{dC_2}$ being maximized. Since Φ is the CDF of a standard normal distribution and $\omega > 0$, we must have that this is $0 \le P_x \le 0.5$. This implies that the probability of CR&PR classification cannot be above 50 % at this target concentration.

As seen in Fig. 2 a drug exposure can exist that maximizes the probability that a patient is classified as SD. The following proposition provides an analytical equation for this concentration and conditions for its existence.

Proposition 3. *There exists a unique $C_i > 0$, $i = 1, \cdots, M$, that maximizes the probability of SD classification (third expression in Eq. (9) if and only if* $a_i > 0$, *and* $Q_i < \frac{-(\log(0.7)+\log(1.2))+\sqrt{(\log(1.2)-\log(0.7))^2+\left(2Tk_g^m e^{-\omega^2}\right)^2}}{2R_iT}$, *where* $Q_i = \sum_{j\neq i} a_jC_j + \sum_{j,k\neq i}\gamma_{jk}C_jC_k$ *and* $R_i = (a_i + \sum_{j=1}^{M}\gamma_{ij}C_j)$.

Moreover, this maximum point is given by,

$$C_i = \frac{-(2TQ_i + \log(0.7) + \log(1.2)) + \sqrt{(\log(1.2) - \log(0.7))^2 + \left(2Tk_g^m e^{-\omega^2}\right)^2}}{2R_i T}, \tag{16}$$

The proof of the proposition can be found in the Appendix.

Applying Proposition 3 with $M = 2$ gives the following relationship between the average concentrations of the two drugs that maximize the probability of SD,

$$C_2 = \frac{-(2Ta_1C_1 + \log(0.7) + \log(1.2)) + \sqrt{(\log(1.2) - \log(0.7))^2 + \left(2Tk_g^m e^{-\omega^2}\right)^2}}{2(a_1 + \gamma_{12}C_2)T}. \tag{17}$$

There are some similarities between this expression and the one from Proposition 2. (Eq. (15). However it is not immediately clear how these relate to each other but the following corollary elucidates this.

Corollary 1. *Call the target concentrations in Propositions 2 and 3 for C_2^{T2} and C_2^{T3}, respectively. By using the standard and reverse triangle inequality we can place an upper and lower bound on C_2^{T2}, which involves C_2^{T3}, for a fixed C_1.*

Writing $X^2 = (\log(1.2) - \log(0.7))^2$ and $Y^2 = \left(2Tk_g^m e^{-\omega^2}\right)^2$, we have that,

$$\begin{aligned} C_2^{T3} &= \frac{-(2Ta_1C_1 + \log(0.7) + \log(1.2)) + \sqrt{X^2 + Y^2}}{2(a_1 + \gamma_{12}C_2)T} \leq \\ &\frac{-(2Ta_1C_1 + \log(0.7) + \log(1.2)) + X + Y}{2(a_1 + \gamma_{12}C_2)T} = \\ &= \frac{-(2Ta_1C_1 + \log(0.7) + \log(1.2)) + (\log(1.2) - \log(0.7)) + 2Tk_g^m e^{-\omega^2}}{2(a_1 + \gamma_{12}C_2)T} = \\ &= \frac{-(2Ta_1C_1 + 2\log(0.7)) + \left(2Tk_g^m e^{-\omega^2}\right)}{2(a_1 + \gamma_{12}C_2)T} = \frac{k_g^m e^{-\omega^2} - \frac{\log(0.7)}{T} - a_1C_1}{(a_1 + \gamma_{12}C_2)} = C_2^{T2} \end{aligned} \tag{18}$$

A similar calculation using the reverse triangle inequality shows that

$$C_2^{T3} \leq C_2^{T4} + \frac{\log(1.2) - \log(0.7)}{T(a_1 + \gamma_{12}C_2)}. \tag{19}$$

Thus, we have that

$$C_2^{T4} \leq C_2^{T3} \leq C_2^{T4} + \frac{\log(1.2) - \log(0.7)}{T(a_1 + \gamma_{12}C_2)},$$

or

$$0 \leq C_2^{T3} - C_2^{T4} \leq \frac{\log(1.2) - \log(0.7)}{T(a_1 + \gamma_{12}C_2)}.$$

2.4. Sensitivity analysis

To gain further insight into the mathematical model we perform the first step in a sensitivity analysis by differentiating the probability functions presented in Lemma 1 with respect to k_g and a_i. The derivative of $P_{CR\&PR}$ with respect to a_i is given by,

$$\frac{\partial(P_{CR\&PR}(a_i))}{\partial a_i} = \frac{\partial\Phi\left(\log\left(\frac{\log(0.7)}{T} + S\right)\Big/\omega\right)}{\partial a_i} = \frac{C_i e^{-\log^2\frac{\left(\frac{\log(0.7)}{T} + S\right)}{k_g^m}}}{\sqrt{2\pi}\omega\left(\frac{\log(0.7)}{T} + S\right)}. \tag{20}$$

To find the derivative with respect to k_g^m we utilize the chain rule and end up with,

$$\frac{\partial\left(P_{CR\&PR}\left(k_g^m\right)\right)}{\partial k_g^m} = \frac{\partial\Phi\left(\log\left(\frac{\log(0.7)}{T} + S\right)\Big/\omega\right)}{\partial k_g^m} = -\frac{e^{-\log^2\frac{\left(\frac{\log(0.7)}{T} + S\right)}{k_g^m}}}{\sqrt{2\pi}\omega k_g^m}. \tag{21}$$

The derivatives of the other categories are found through similar calculations.

3. Discussion

The first step in our analytical analysis consists of deriving predictions of RECIST response (Eq. (9) for a commonly used TGI model assuming that the average drug concentrations drive the model and that the growth rate is log-normally distributed. A similar derivation is possible for a large number of other models as long as they have an analytical solution and the chosen parameter distributions result in tractable CDF. The log-normal distribution is often a good choice for these types of growth parameters when analyzing data in oncology. However, often when a log-normally distributed random variable is transformed, *e.g.,* by addition to another log-normally distributed random variable, the resulting CDF does not have an analytical solution (Ben Hcine, 2014). Using a normal distribution instead would lead to simpler expressions and allow for more parameters in the model to be distributed. Hence, this could be interesting to investigate as well.

In the case of additive log-normal variables, the resulting CDF can be approximated with, *e.g.,* the Fenton-Wilkinsson approximation (Cobb et al., 2012). Thus, in this case, approximate analytical expressions can still be derived. However, more importantly, even though we cannot derive exact analytical expressions for models with more than one log-normally distributed parameter, approximations can still be found through Monte Carlo simulations.

All our predictions are based on the criteria for target progression, however, in a clinical trial, a patient can also be assigned as PD due to non-target progression, *e.g.,* due to the appearance of new tumor lesions. Previous research has established a correlation between these two types of progression, using either a sequential or joint modeling approach (Claret et al., 2009; Yu et al., 2020). In the joint modeling approach, the predictions from the TGI model correlate with the probability of non-target progression. Thus, it is possible to continue the analysis presented in this paper by incorporating predictions of non-target progression.

In dynamical system modeling of combination therapies, it is common that the efficacy of the combination of drugs A and B is the summation of the efficacy of the two respective drugs given as monotherapies and a potential interaction term (Cardilin et al., 2017; Gabrielsson et al., 2016; Koch et al., 2009; Pierrillas et al., 2018; Vakil and Trappe, 2019). This naturally leads to the idea of equivalent exposures, *e.g.,* TSE, where the exposure reduction of one drug can be compensated by an increase in exposure of the other drug, while still achieving the desired treatment outcome. However, a popular hypothesis for explaining the benefit seen in progression-free survival (the time PD occurs) and response rates ($P_{CR\&PR}$) of combination therapies is that of independent drug action (Palmer and Sorger, 2017; Plana et al., 2022; Sun et al., 2021). The idea is that the response for a specific individual given both drugs A and B is the best/maximum of the respective monotherapies, where the correlation between them is also considered.

Both of these approaches have been shown to fit data and have predictive capabilities but are fundamentally different. The probabilistic expression we present directly connects the dynamical model to the two clinical endpoints and could thus be used to better understand these findings. This is, however, outside the scope of this paper but is a highly interesting topic for future work. The first step in this would be to perform the derivations again but this time assuming that the drug sensitivity is patient-specific.

3.1. Sample size

With Theorem 1 we establish a method for predicting the necessary sample size for comparing two treatments given a specific significance level and test power. The strength of this method is that it links the sample size with model parameters, such as the drug exposure, and can thus answer questions such as: If we change the treatment schedule how many more/fewer subjects do we need to recruit? Another example of its use could be to determine what drug dose, within the therapeutic range (Cooney et al., 2017), two treatments should be tested against each

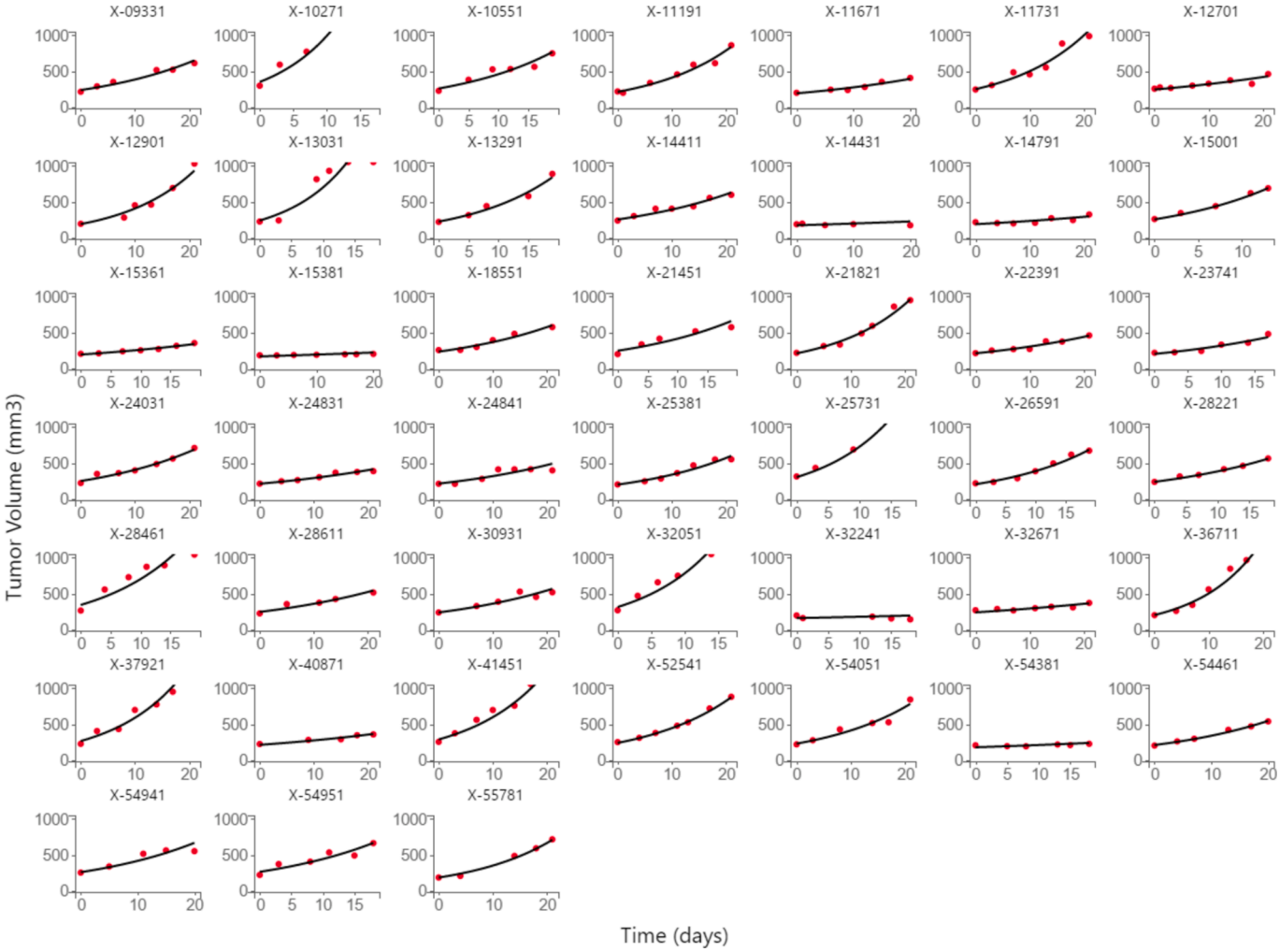

Fig. A1. Individuals fits for the untreated group. Red dots are the experimental data and black lines the model predictions.

other at to most likely find a significant difference or to minimize the number of patients.

3.2. Target exposure

Treatment time is an important parameter in RECIST classification, but it does not affect the TSE predictions. Moreover, as TSE only predicts tumor growth or shrinkage, it is not possible to use this tool to predict the clinically relevant SD category. Thus, we believe that TSE is not entirely appropriate as a target exposure for clinical studies.

To remedy these shortcomings of TSE, we derived a similar target exposure that can be viewed as an extension of the classical TSE concept. The target exposure is derived in Proposition 1 and is more suited for clinical predictions since it is both affected by the treatment time, T, and allows for predictions of all RECIST categories. A further benefit is that it is affected when model parameters are scaled, which gives this new tool more translational relevance than TSE. Moreover, as the treatment time approaches infinity the predictions converge to the TSE predictions, i.e., TSE can be seen as the steady-state solution to this new prediction tool.

We also derived two other potentially interesting exposure expressions. The first maximizes the derivative of $P_{CR\&PR}$, *i.e.,* at what exposure does an increase in drug exposure have the highest benefit for the patient. As we previously mentioned, the $P_{CR\&PR}$ where this has to occur cannot be above 0.5. Therefore, drug combinations that are not tolerable at these exposure levels are predicted to not reach clinical efficacy above this. Depending on the severity of the disease, this may give an indication of what drugs to disregard for future study.

The second exposure expression maximizes the probability that a patient is classified as SD and is similar to TSE in that both, in a sense, aim for tumor homeostasis. Even though SD is not the best patient response, it has been shown to correlate with improvements in disease-related symptoms and quality of life (Kelly, 2003). Aiming for SD could thus strike a balance between efficacious treatment and toxicological effects and could potentially be used to give an idea of an appropriate starting exposure for dose-escalation phase I studies.

3.3. Sensitivity analysis

The sensitivity expressions with respect to the two types of model rate parameters, k_g and a_i, are shown in Eqs. (20) and (21). Since these parameters are candidates for inter-species translational scaling or replacement, these expressions could potentially be used to better understand how the scaling/replacement affects the model dynamics. This could facilitate the search for a better way of scaling these types of semi-mechanistic tumor models that better capture the inter-species differences. If successful, this would make sure that fewer clinically inefficacious drugs enter the clinical development stage.

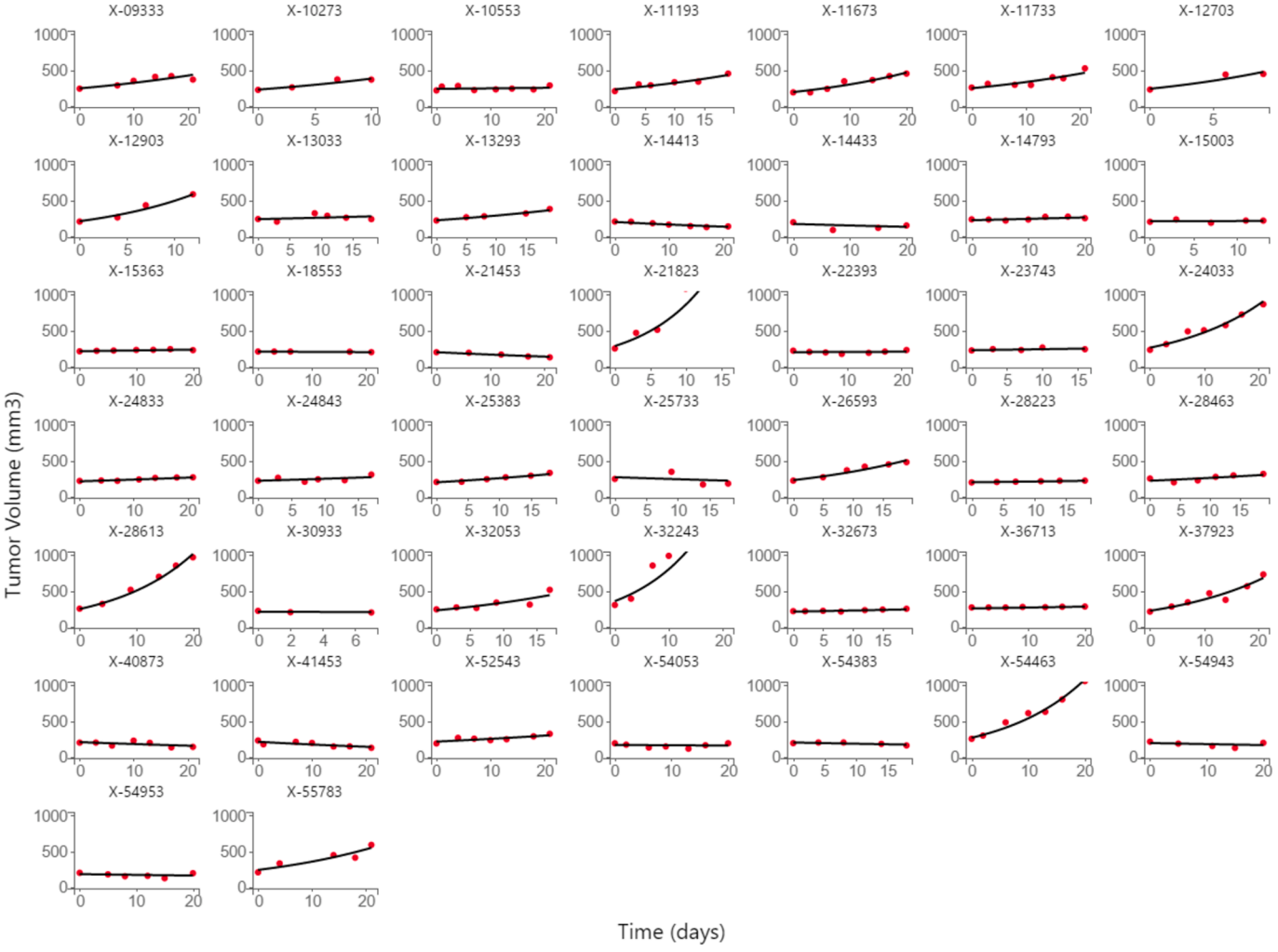

Fig. A2. Individuals fits for the binimetinib group. Red dots are the experimental data and black lines the model predictions.

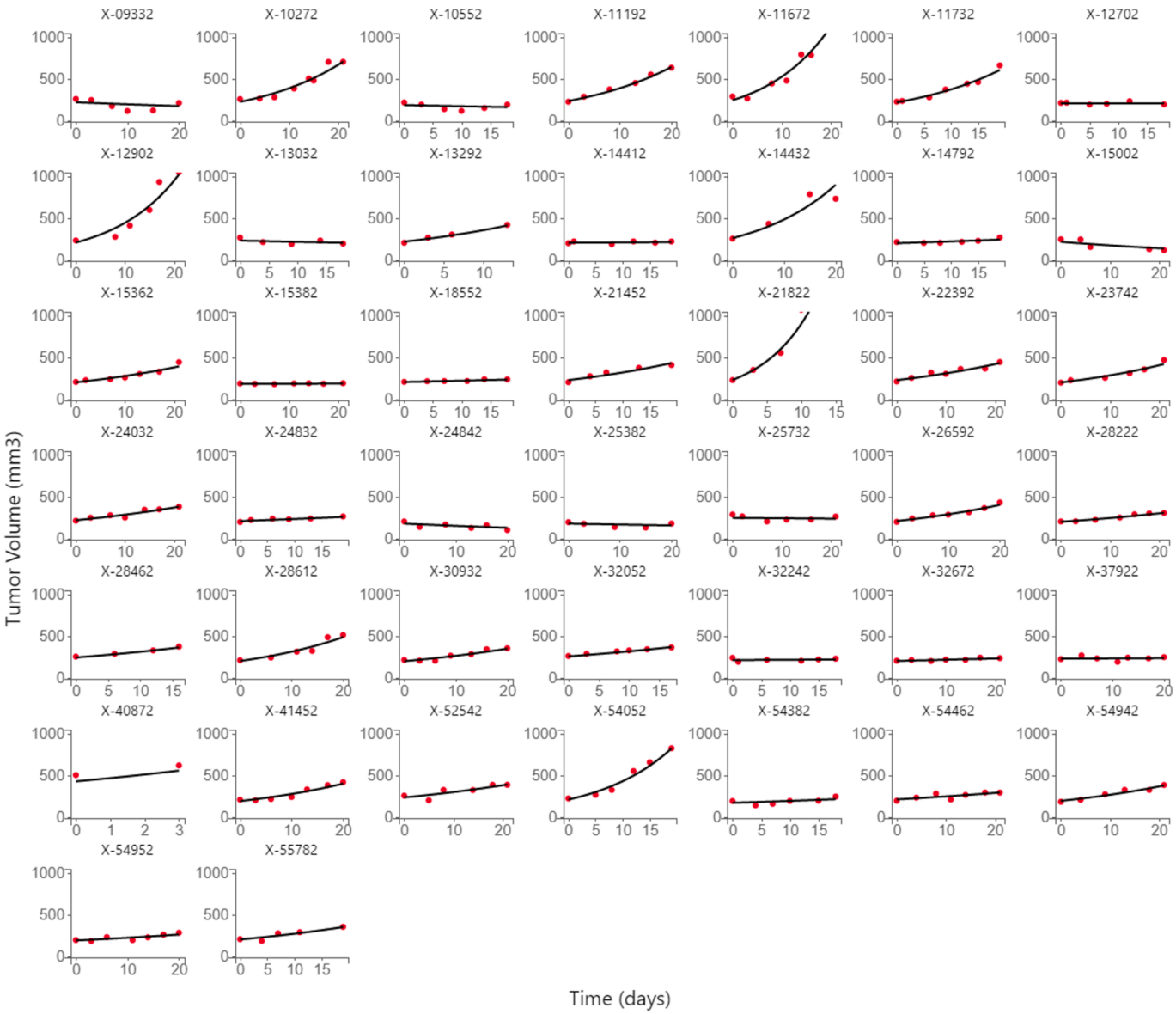

Fig. A3. Individuals fits for the BYL719 group. Red dots are the experimental data and black lines the model predictions.

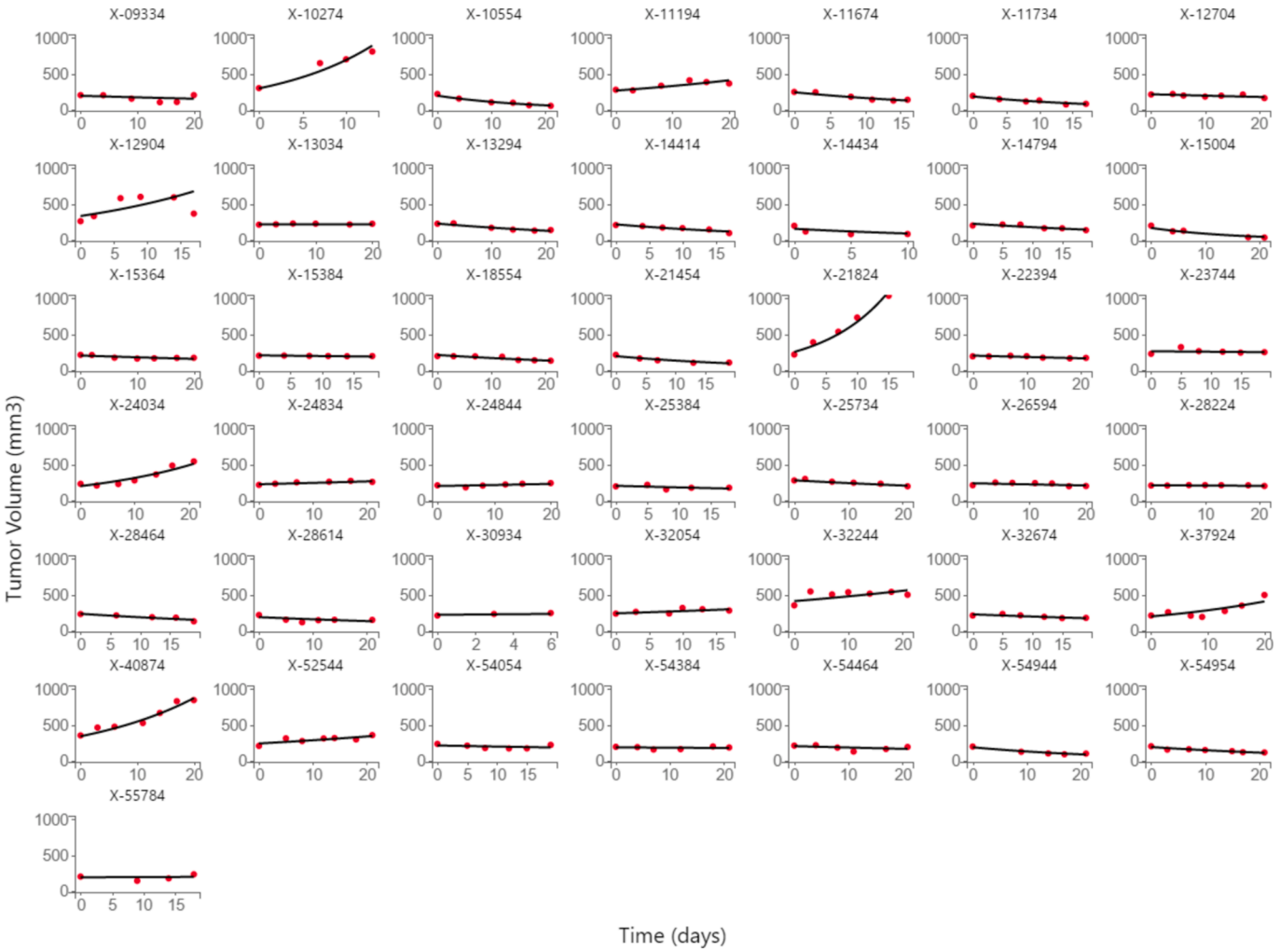

Fig. A4. Individuals fits for the combination group. Red dots are the experimental data and black lines the model predictions.

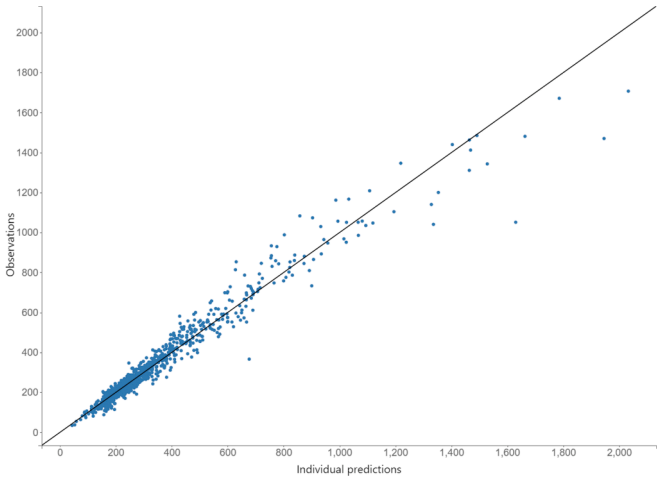

Fig. A5. Observations (tumor volume) plotted against model predictions.

4. Conclusions

We derived probabilistic expressions from a commonly used TGI model describing the proportion of patients categorized in each RECIST category. The expressions were used to predict the necessary sample size required to achieve a certain significance level and test power. The expressions were also used to derive equations for the necessary exposure combinations of two drugs that result in a certain proportion of patients being categorized in each RECIST category. This can be seen as an extension of the classical TSE concept.

Furthermore, two other exposure equations were derived using the same probabilistic expression. The first describes when an increased drug concentration is predicted to be most beneficial to the patients and the second at what concentration level a patient is most likely classified as SD. Preclinical data was also analyzed using the presented model and the parameter estimates were used to illustrate the analytical results. Finally, to facilitate translational research we also present the sensitivity of the RECIST predictions with respect to the model parameters.

CRediT authorship contribution statement

Marcus Baaz: Conceptualization, Data curation, Formal analysis, Investigation, Methodology, Validation, Visualization, Writing – original draft, Writing – review & editing. **Tim Cardilin:** Conceptualization, Formal analysis, Investigation, Methodology, Supervision, Validation, Writing – original draft, Writing – review & editing. **Torbjörn Lundh:** Conceptualization, Formal analysis, Supervision, Writing – original draft, Writing – review & editing. **Mats Jirstrand:** Conceptualization, Formal analysis, Funding acquisition, Investigation, Project administration, Resources, Supervision, Writing – original draft, Writing – review & editing.

Fig. A6. Individual weighted residual (IWRES) plotted against time (left) and tumor volume (right).

Declaration of competing interest

The authors declare that they have no known competing financial interests or personal relationships that could have appeared to influence the work reported in this paper.

Marcus Baaz was supported by an educational research grant from Merck KGaA, Darmstadt, Germany (CrossRef Funder ID: 10.13039/100009945).

Appendix

Concentration Dynamics Analysis.

In the main analysis, we let the average drug concentration drive the pharmacodynamic response. Here we show that the analysis can also be performed using both a dynamical concentration model and a repeated dosing schedule.

Assume that drugs are given with a repeated dosing schedule where $s = (s_1, s_2, \cdots, s_N)$ are the days the drugs are given to patients, and that the concentration dynamics are given by, See Figs. A1-A6

$$C_i(t) = \sum_{j=1}^{N} C_{0,i} e^{-k_{e,i}t} H(t - s_j),$$

where H is the Heaviside function and $C_{0,i}$ and $k_{e,i}$ are the initial concentration and elimination rate of drug i, respectively.

The integral of the monotherapy terms in Eq. (2), then becomes

$$\int_0^t a_i \mathrm{C_i}(\mathrm{t}) \mathrm{d}\tau = a_i C_{0,i} \int_0^t \sum_{j=1}^{N} e^{-k_{e_i}(\tau - s_j)} H(\tau - s_j) d\tau,$$

$$= a_i C_{0,i} \sum_{j=1}^{N} e^{k_{e,i} s_j} \int_{s_j}^{t} e^{-k_{e,i}\tau} d\tau H(t - s_j),$$

$$= \frac{a_i C_{0,i}}{k_{e,i}} \sum_{j=1}^{N} e^{k_{e,i} s_j} (1 - e^{-k_{e,i}t}) H(t - s_j).$$

For the interaction terms we have,

$$\int_0^t \gamma_{ik} \mathrm{C_i}(\mathrm{t}) \mathrm{C_k}(\mathrm{t}) \mathrm{d}\tau = \int_0^t \sum_{j=1}^{N} \gamma_{ik} e^{-k_{e,i}(\tau - s_j)} e^{-k_{e,k}(\tau - s_j)} H(\tau - s_j) H(\tau - s_j) d\tau$$

$$= \gamma_{ik} C_{0,i} C_{0,k} \sum_{j=1}^{N} e^{(k_{e,i}+k_{e,k})s_j} \int_{s_j}^{t} e^{-(k_{e,i}+k_{e,k})\tau} d\tau H(t-s_j),$$

$$= \frac{\gamma_{ik} C_{0,i} C_{0,k}}{k_{e,i}+k_{e,k}} \sum_{j=1}^{N} e^{(k_{e,i}+k_{e,k})s_j} (1 - e^{-(k_{e,i}+k_{e,k})t}) H(t-s_j).$$

Thus, we can see that given a treatment schedule and knowledge of the drug dynamics, in this case $k_{e,i}$ and $C_{0,i}$, all these integrals will reduce to scalar values multiplied by the potency/interaction parameter.

Model Validation plots.

Proof of Lemma 1.

We introduce the assumption that k_g is log-normally distributed to Eq. (8) and find the sought probabilities by considering the distribution of η. Using Eq. (8), the probability for CR&PR classification can be written as,

$$P_{\text{CR\&PR}} = P\left(100\%\left(e^{(k_g^m e^{\eta} - S)T} - 1\right) \leq -30\%\right) = P\left((k_g^m e^{\eta} - S)T \leq \log(0.7)\right) = P\left(\eta \leq \chi_{\frac{\log(0.7)}{T}+S)>0} \log\left(\frac{\frac{\log(0.7)}{T}+S}{k_g^m}\right)\right)$$

$$= \chi_{\frac{\log(0.7)}{T}+S>0}\, \phi\left(\log\left(\frac{\frac{\log(0.7)}{T}+S}{k_g^m}\right) \Big/ \omega\right), \tag{A1}$$

where χ is an indicator function. A similar calculation shows that the probability for PD classification is given by,

$$P_{PD} = P\left(100 e^{\left(k_g^m e^{\eta} - S\right)T} - 100 \geq 20\right) = 1 - \phi\left(\frac{\log\left(\frac{\frac{\log(1.2)}{T}+S}{k_g^m}\right)}{\omega}\right). \tag{A2}$$

Since SD occurs if neither CR&PR nor PD has been achieved, we have that,

$$P_{SD} = 1 - P_{CR\&PR} - P_{PD} = \Phi\left(\frac{\log\left(\frac{\frac{\log(1.2)}{T}+S}{k_g^m}\right)}{\omega}\right) - \chi_{\frac{\log(0.7)}{T}+S>0}\, \Phi\left(\frac{\log\left(\frac{\frac{\log(0.7)}{T}+S}{k_g^m}\right)}{\omega}\right). \tag{A3}$$

Proof of Proposition 3

Assume that $a_i > 0$ and Q_i is sufficiently small for there to exist $C_i \in \mathscr{R}^+$ such that $P_{CR\&PR}(C_i) \neq 1$. Then there exists $C_i \in \mathscr{R}^+$ such that $P_{SD}(C_i) > 0$. Moreover, using the CDF of the normal distribution and Eq. (9) (third expression), we have that,

$$\lim_{C_i \to \infty} P_{SD}(C_i) = 0,$$

and $P_{SD} \leq 1 \ \forall C_i \in \mathscr{R}^+$. Therefore, there has to exist at least one maximum point of P_{SD} on $\mathscr{R}^+$. The maximum point has to be either $C_i = 0$ or one of the extreme points. We find all extreme points by solving $\frac{\partial(P_{SD}(C_i))}{\partial C_i} = 0$.

We assume that $\frac{\log(0.7)}{T} + S > 0$. Using the chain rule and the fact that the derivative of a CDF is the PDF we have that,

$$\frac{\partial(P_{CR\&PR}(C_i))}{\partial C_i} = \frac{\partial \Phi\left(\frac{\log\left(\frac{\frac{\log(0.7)}{T}+S}{k_g^m}\right)}{\omega}\right)}{\partial C_i} = \frac{\left(a_i + \sum_{j=1}^{M} \gamma_{ij} C_j\right) e^{-\log^2 \frac{\left(\frac{\log(0.7)}{T}+S\right)}{k_g^m}}}{\sqrt{2\pi}\omega\left(\frac{\log(0.7)}{T}+S\right)}. \tag{A4}$$

Similarly, we have,

$$\frac{\partial(P_{PD}(C_i))}{\partial C_i} = -\frac{\partial\Phi\left(\frac{\log\left(\frac{\log(1.2)}{T}+S\right)}{k_g^m}\right)}{\partial C_i} = \frac{R_i e^{-\log^2\frac{\left(\frac{\log(1.2)}{T}+S\right)}{k_g^m}}}{\sqrt{2\pi}\omega\left(\frac{\log(1.2)}{T}+S\right)}, \tag{A5}$$

and thus,

$$\frac{\partial(P_{SD}(C_i))}{\partial C_i} = \frac{R_i}{\sqrt{2\pi}\omega}\left(\frac{e^{-\log^2\frac{\left(\frac{\log(1.2)}{T}+S\right)}{k_g^m}}}{\left(\frac{\log(1.2)}{T}+S\right)} - \frac{e^{-\log^2\frac{\left(\frac{\log(0.7)}{T}+S\right)}{k_g^m}}}{\left(\frac{\log(0.7)}{T}+S\right)}\right). \tag{A6}$$

To find the extreme points, we put the right-hand side of Eq. A(6) equal to zero. Since $\frac{1}{x} = e^{-\log(x)}$, we have,

$$e^{-\log^2\frac{\left(\frac{\log(1.2)}{T}+S\right)}{k_g^m}-\log\left(\frac{\log(1.2)}{T}+S\right)} = e^{-\log^2\frac{\left(\frac{\log(0.7)}{T}+S\right)}{k_g^m}-\log\left(\frac{\log(0.7)}{T}+S\right)}. \tag{A7}$$

Taking the logarithm of both sides yields,

$$\frac{\log^2\left(\frac{\log(0.7)}{T}+S\right)}{2\omega^2}+\log\left(\frac{\log(0.7)}{T}+S\right) = \frac{\log^2\left(\frac{\log(1.2)}{T}+S\right)}{2\omega^2}+\log\left(\frac{\log(1.2)}{T}+S\right). \tag{A8}$$

Writing $X = \log\left(\frac{\log(0.7)}{T}+S\right)$ and $Y = \log\left(\frac{\log(1.2)}{T}+S\right)$, we have that,

$$\frac{X^2}{2\omega^2}+X = \frac{Y^2}{2\omega^2}+Y. \tag{A9}$$

Solving Eq. A(9) for X we have that,

$$X = -\omega^2 \pm \sqrt{\omega^4+Y^2+2Y\omega^2}. \tag{A10}$$

Since $\omega^4 + Y^2 + 2Y\omega^2 = (\omega^2+Y)^2$, we have that,

$X_1 = Y,$

$X_2 = -2\omega^2 - Y.$

However, since $\log(0.7) \neq \log(1.2)$, $X \neq Y$, thus, X_2 is the only valid root. Reinserting the definitions of X and Y into the second root, we have that,

$$\log\left(\frac{\log(0.7)}{T}+S\right) = -2\omega^2 - \log\left(\frac{\log(1.2)}{T}+S\right),$$

$$\log\left(\frac{\left(\frac{\log(0.7)}{T}+S\right)\left(\frac{\log(1.2)}{T}+S\right)}{(k_g^m)^2}\right) = -2\omega^2,$$

$$\frac{\left(\frac{\log(0.7)}{T}+S\right)\left(\frac{\log(1.2)}{T}+S\right)}{(k_g^m)^2}-e^{-2\omega^2}=0.$$

Reinserting the definition of S and solving this equation for C_i yields,

$$C_i=\frac{-(2\,T\,Q_i+\log(0.7)+\log(1.2))\pm\sqrt{(\log(1.2)-\log(0.7))^2+\left(2\,T k_g^m e^{-\omega^2}\right)^2}}{2\,R_i\,T}. \tag{A11}$$

Since $\log(0.7)+\log(1.2)<0$, we have,

$$C_i=\frac{-(2\,T\,Q_i+\log(0.7)+\log(1.2))-\sqrt{(\log(1.2)-\log(0.7))^2+\left(2\,T k_g^m e^{-\omega^2}\right)^2}}{2\,R_i\,T}<0, \tag{A12}$$

and therefore this solution is not a valid concentration. The other root,

$$C_i=\frac{-(2\,T\,Q_i+\log(0.7)+\log(1.2))+\sqrt{(\log(1.2)-\log(0.7))^2+\left(2\,T k_g^m e^{-\omega^2}\right)^2}}{2\,R_i\,T}, \tag{A13}$$

can be both negative and positive depending on Q_i. Therefore, there exists at most one extreme point on $\mathscr{R}^+$. Thus, for certain Q_i Eq. A13 is positive and the first part of the proof is complete. The next step in the proof is to determine what restriction has to be put on Q_i for Eq. A13 to be positive.

There exist no extreme points on $\mathscr{R}^+$ if and only if $\frac{\partial(P_{SD}(0))}{\partial C_i}<0$, since $\lim_{C_i\to\infty}P_{SD}(C_i)=0$, $P_{SD}(0)>0$, and there exists at most one extreme point on $\mathscr{R}^+$. Conversely, if and only if $\frac{\partial(P_{SD}(0))}{\partial C_i}>0$ an extreme point exists on $\mathscr{R}^+$. Therefore, we can find a criterion on Q_i such that $\frac{\partial(P_{SD}(0))}{\partial C_i}>0$.

From Eq. A13, we have that,

$$C_i+\frac{Q_i}{R_i}=\frac{-(\log(0.7)+\log(1.2))+\sqrt{(\log(1.2)-\log(0.7))^2+\left(2\,T k_g^m\,e^{-\omega^2}\right)^2}}{2\,R_i\,T} \tag{A14}$$

Putting $C_i=0$, we then have an equation for $\frac{\partial(P_{SD}(0))}{\partial C_i}=0$,

$$Q_i=\frac{-(\log(0.7)+\log(1.2))+\sqrt{(\log(1.2)-\log(0.7))^2+\left(2\,T k_g^m\,e^{-\omega^2}\right)^2}}{2\,T}, \tag{15}$$

and thus, if $Q_i<\frac{-(\log(0.7)+\log(1.2))+\sqrt{(\log(1.2)-\log(0.7))^2+\left(2k_g^m e^{-\omega^2}\right)^2}}{2T}$, then $\frac{\partial(P_{SD}(0))}{\partial C_i}>0$ and the extreme point given by Eq. A13 has to be the unique concentration that maximizes P_{SD}.■

References

Al-Lazikani, B., Banerji, U., Workman, P., 2012. Combinatorial drug therapy for cancer in the post-genomic era. Nat Biotechnol. 30 (7), 679–692.

Ben Hcine M, Bouallegue R. Fitting the Log Skew Normal to the Sum of Independent Lognormals Distribution. In: Computer Science & Information Technology (CS & IT) [Internet]. Academy & Industry Research Collaboration Center (AIRCC); 2014 [cited 2021 Nov 9]. p. 54–68. Available from: http://www.airccj.org/CSCP/vol4/csit43105.pdf.

Broxmeyer, H., 2020 Jun 19. Players in Drug-Resistant Leukemia Stem/Initiating Cells and Immunity in Patients with CML in Context of Oxygen Levels: Would Collecting/Processing Cells in Hypoxia Offer Additional Information? A Next Frontier of Investigation. Blood Cancer Discovery. 1 (1), 13–15.

Cardilin, T., Almquist, J., Jirstrand, M., Sostelly, A., Amendt, C., El Bawab, S., et al., 2017. Tumor Static Concentration Curves in Combination Therapy. AAPS J. 19 (2), 456–467.

Center for Drug Evaluation and Research. Multi-Disciplinary Review and Evaluation NDA 210498 MEKTOVI™. 2015.

Center for Drug Evaluation and Research. Pharmacology Review of Alpelisib. 2018.

Choo, E.F., Ng, C.M., Berry, L., Belvin, M., Lewin-Koh, N., Merchant, M., et al., 2013. PK-PD modeling of combination efficacy effect from administration of the MEK inhibitor GDC-0973 and PI3K inhibitor GDC-0941 in A2058 xenografts. Cancer Chemother Pharmacol. 71 (1), 133–143.

Claret, L., Girard, P., Hoff, P.M., Van Cutsem, E., Zuideveld, K.P., Jorga, K., et al., 2009. Model-Based Prediction of Phase III Overall Survival in Colorectal Cancer on the Basis of Phase II Tumor Dynamics. Journal of Clinical Oncology. 27 (25), 4103–4108.

Cobb, B., Rumí, R., Salmerón, A., 2012. Approximating the Distribution of a Sum of Log-normal Random Variables. In.

Cooney, L., Loke, Y.K., Golder, S., Kirkham, J., Jorgensen, A., Sinha, I., et al., 2017 Jun. Overview of systematic reviews of therapeutic ranges: methodologies and recommendations for practice. BMC Med Res Methodol. 2 (17), 84.

Delyon, B., Lavielle, M., Moulines, E., 1999. Convergence of a Stochastic Approximation Version of the EM Algorithm. The Annals of Statistics. 27 (1), 94–128.

Eisenhauer, E.A., Therasse, P., Bogaerts, J., Schwartz, L.H., Sargent, D., Ford, R., et al., 2009. New response evaluation criteria in solid tumours: Revised RECIST guideline (version 1.1). European Journal of Cancer. 45 (2), 228–247.

Gabrielsson, J., Gibbons, F.D., Peletier, L.A., 2016. Mixture dynamics: Combination therapy in oncology. European Journal of Pharmaceutical Sciences. 88, 132–146.

Gao, H., Korn, J.M., Ferretti, S., Monahan, J.E., Wang, Y., Singh, M., et al., 2015. High-Throughput Screening Using Patient-Derived Tumor Xenografts to Predict Clinical Trial Drug Response. Nature Medicine. 21 (11), 1318–1325.

Goteti, K., Garner, C.E., Utley, L., Dai, J., Ashwell, S., Moustakas, D.T., et al., 2010. Preclinical pharmacokinetic/pharmacodynamic models to predict synergistic effects of co-administered anti-cancer agents. Cancer Chemother Pharmacol. 66 (2), 245–254.

Hemminki, K., Försti, A., Liska, V., Kanerva, A., Hemminki, O., Hemminki, A., 2023. Long-term survival trends in solid cancers in the Nordic countries marking timing of improvements. International Journal of Cancer. 152 (9), 1837–1846.

Jacobs, P., 1997 Aug 1. Myelodysplasia nd the leukemias. Disease-a-Month. 43 (8), 507–597.

Jumbe, N.L., Xin, Y., Leipold, D.D., Crocker, L., Dugger, D., Mai, E., et al., 2010. Modeling the efficacy of trastuzumab-DM1, an antibody drug conjugate, in mice. J Pharmacokinet Pharmacodyn. 37 (3), 221–242.

Kelly K. The benefits of achieving stable disease in advanced lung cancer. Oncology (Williston Park). 2003 Jul;17(7):957–63; discussion 963, 968–70.

Koch, G., Walz, A., Lahu, G., Schropp, J., 2009. Modeling of tumor growth and anticancer effects of combination therapy. J Pharmacokinet Pharmacodyn. 36 (2), 179–197.

Koga, Y., Ochiai, A., 2019. Systematic Review of Patient-Derived Xenograft Models for Preclinical Studies of Anti-Cancer Drugs in Solid Tumors. Cells. 8 (5), 418.

Leander, J., Almquist, J., Johnning, A., Larsson, J., Jirstrand, M., 2021. Nonlinear Mixed Effects Modeling of Deterministic and Stochastic Dynamical Systems in Wolfram Mathematica. IFAC-PapersOnLine. 54 (7), 409–414.

Miao, X., Koch, G., Straubinger, R.M., Jusko, W.J., 2016. Pharmacodynamic modeling of combined chemotherapeutic effects predicts synergistic activity of gemcitabine and trabectedin in pancreatic cancer cells. Cancer Chemother Pharmacol. 77 (1), 181–193.

Monolix 2021R2, Lixoft SAS, a Simulations Plus company. Lixoft SAS, a Simulations Plus company.

Ouerdani, A., Struemper, H., Suttle, A.B., Ouellet, D., Ribba, B., 2015. Preclinical Modeling of Tumor Growth and Angiogenesis Inhibition to Describe Pazopanib Clinical Effects in Renal Cell Carcinoma. CPT: Pharmacometrics & Systems. Pharmacology. 4 (11), 660–668.

Palmer, A.C., Sorger, P.K., 2017 Dec 14. Combination Cancer Therapy Can Confer Benefit via Patient-to-Patient Variability without Drug Additivity or Synergy. Cell. 171 (7), 1678–1691.e13.

Park, J.W., Kerbel, R.S., Kelloff, G.J., Barrett, J.C., Chabner, B.A., Parkinson, D.R., et al., 2004. Rationale for Biomarkers and Surrogate End Points in Mechanism-Driven Oncology Drug Development. Clin Cancer Res. 10 (11), 3885–3896.

Pierrillas, P.B., Fouliard, S., Chenel, M., Hooker, A.C., Friberg, L.F., Karlsson, M.O., 2018. Model-Based Adaptive Optimal Design (MBAOD) Improves Combination Dose Finding Designs: An Example in Oncology. The AAPS Journal. 20 (2), 39.

Plana, D., Palmer, A.C., Sorger, P.K., 2022 Mar 1. Independent Drug Action in Combination Therapy: Implications for Precision Oncology. Cancer Discov. 12 (3), 606–624.

Ribba, B., Kaloshi, G., Peyre, M., Ricard, D., Calvez, V., Tod, M., et al., 2012. A Tumor Growth Inhibition Model for Low-Grade Glioma Treated with Chemotherapy or Radiotherapy. Clinical Cancer Research. 18 (18), 5071–5080.

Ribba, B., Holford, N.H., Magni, P., Trocóniz, I., Gueorguieva, I., Girard, P., et al., 2014 May. A Review of Mixed-Effects Models of Tumor Growth and Effects of Anticancer Drug Treatment Used in Population Analysis. CPT: Pharmacometrics & Systems. Pharmacology. 3 (5), e113.

Sakpal, T.V., 2010. Sample Size Estimation in Clinical Trial. Perspect Clin Res. 1 (2), 67–69.

Sun, L.Z., Wu, C., Li, X., Chen, C., Schmidt, E.V., 2021 Jul. Independent action models and prediction of combination treatment effects for response rate, duration of response and tumor size change in oncology drug development. Contemporary Clinical Trials. 1 (106), 106434.

Sung, H., Ferlay, J., Siegel, R.L., Laversanne, M., Soerjomataram, I., Jemal, A., et al., 2021. Global Cancer Statistics 2020: GLOBOCAN Estimates of Incidence and Mortality Worldwide for 36 Cancers in 185 Countries. CA: A Cancer Journal for Clinicians. 71 (3), 209–249.

Vakil, V., Trappe, W., 2019. Drug Combinations: Mathematical Modeling and Networking Methods. Pharmaceutics. 11 (5), 208.

Wang, H., China, P.R., 2007. Sample Size Calculation for Comparing Proportions. In Wiley Encyclopedia of. Clinical Trials.

Yin, A., Moes, D.J.A.R., van Hasselt, J.G.C., Swen, J.J., Guchelaar, H., 2019 Oct. A Review of Mathematical Models for Tumor Dynamics and Treatment Resistance Evolution of Solid Tumors. CPT Pharmacometrics Syst Pharmacol. 8 (10), 720–737.

Yu, J., Wang, N., Kågedal, M., 2020. A New Method to Model and Predict Progression Free Survival Based on Tumor Growth Dynamics. CPT: Pharmacometrics & Systems. Pharmacology. 9 (3), 177–184.

Zettler, M.E., Lee, C.H., Gajra, A., Feinberg, B.A., 2021. Assessment of objective response rate (ORR) by investigator versus blinded independent central review in pivotal trials of drugs approved for solid tumor indications. JCO. May 20;39(15_suppl): e13570–e13570.